A Climatology of Hurricane Eye Formation*

JONATHAN L. VIGH

National Center for Atmospheric Research,+ Boulder, and Department of Atmospheric Science, Colorado State University, Fort Collins, Colorado

JOHN A. KNAFF

Regional and Mesoscale Meteorology Branch, NOAA/NESDIS, Fort Collins, Colorado

WAYNE H. SCHUBERT

Department of Atmospheric Science, Colorado State University, Fort Collins, Colorado

(Manuscript received 29 April 2011, in final form 21 November 2011)

ABSTRACT

This paper presents a climatology of the initial eye formations of a broad set of Atlantic tropical cyclones (TCs) during 1989–2008. A new dataset of structure and intensity parameters is synthesized from the vortex data messages transmitted by routine aircraft reconnaissance. Using these data together with satellite imagery and other established datasets, the times when each TC achieved various stages of eye development are tabulated to form the basis of the climatology. About 60% of Atlantic TCs form eyes. Most often, aircraft observe the eye structure before it appears in IR satellite imagery. Eyes tend to form in high potential intensity environments characterized by high sea surface temperatures and low-to-moderate environmental vertical wind shear. A notable discovery is that most (67%) TCs that form eyes tend to do so within 48 h of the cyclone's reaching tropical storm strength. This suggests the existence of an opportune time window during which a TC can readily form an eye. From the lengths of time taken to reach various stages of eye development, the characteristic time scale for eye formation is estimated to be about 36 h.

1. Introduction

The formation of an eye (and by implication, an eyewall) has long been viewed as the hallmark of a tropical cyclone (TC) that has surpassed the minimum threshold for hurricane intensity [64-kt (33 m s^{-1}) maximum 1-min sustained surface wind speed]. The central calm of the eye, with occasional breaks of clouds, led early researchers to correctly surmise that the eye region must contain descending air (Ballou 1892). As knowledge of hurricane thermodynamics increased, workers noted that the hydrostatic pressure decrease caused by condensational latent heating is insufficient to support the surface pressure drop found in a hurricane (Palmén 1956; Malkus 1958)—the development of an extreme pressure deficit requires adiabatic warming by forced subsidence in the eye (Anthes 1982). Since low surface pressures are critical to enhancing the surface enthalpy fluxes, a TC cannot intensify beyond a certain point without a warm core. Structurally, the intense warming associated with the formation of an eye paves the way for further intensification and organization of the TC.

Observationally, the appearance and definition of an eye figure prominently in the successful Dvorak technique of estimating TC intensity using satellite imagery—the eye structure often becomes evident in satellite imagery when the TC slightly exceeds hurricane intensity (Dvorak 1984). In addition to the observation that TCs readily form eyes near the hurricane threshold, several researchers

* Supplemental information related to this paper is available at the Journals Online website: http://dx.doi.org/10.1175/MWR-D-11-00108.s1.

+ The National Center for Atmospheric Research is sponsored by the National Science Foundation.

Corresponding author address: Dr. Jonathan Vigh, National Center for Atmospheric Research, P. O. Box 3000, Boulder, CO 80307-3000.
E-mail: jvigh@ucar.edu

DOI: 10.1175/MWR-D-11-00108.1

have associated the formation of an eye with a period of rapid intensification (Malkus 1958; Yanai 1961; Mundell 1990; Weatherford and Gray 1988b; Shapiro and Willoughby 1982; Willoughby 1990). These studies suggest that so long as conditions remain favorable, a TC can intensify rapidly once an eye has formed. These concepts and observations lend support to the idea that hurricane structure and intensity are inextricably linked. Whether eye formation causes intensification, or is merely indicative of a chain of processes that lead to intensification, it behooves us to consider the appearance of an eye as an important marker in TC development.

Before undertaking an investigation of the linkages between structure and intensification, we think it prudent to first consider the climatology of hurricane eye formation by examining the characteristics and distributions from a large number of events. Several studies have touched on this subject, albeit peripherally. Weatherford and Gray (1988b) used aircraft data on the 700-mb flight level from 66 western Pacific typhoons to examine several aspects of the relationship between the eye and a TC's intensity, including the resulting intensity change and the size of the eye. Eyes were reported across a wide range of intensities, but were more often observed in intense TCs than in weak TCs. Also, eyes were reported more frequently in intensifying TCs than in weakening TCs. TCs that form eyes early (at lower intensities, e.g., the tropical storm stage) tend to have smaller eyes, while TCs that form eyes later (at higher intensities) tend to have larger eyes. Taken together, their results suggest that the formation of an eye is associated with increasing levels of TC organization.

Kimball and Mulekar (2004) used Extended Best-Track (EBT) data to establish a detailed, quantitative climatology of size parameters for Atlantic TCs, including eye radius, radius of maximum winds, and outer size parameters. Analyzing statistics for the first eye, this study showed that TCs form eyes most frequently at the category-1 hurricane stage. The first eye is reported less frequently in the category-2, -3, and -4 stages, even less frequently in tropical storms, and not at all in tropical depression and category-5 stages. As we discuss later, the EBT data are less than ideal for studying the problem of eye formation.

The steady accumulation of thousands of vortex data messages (VDMs) from routine aircraft reconnaissance missions over the past two decades offers fertile ground from which to grow our knowledge on the subject of eye formation. While these VDMs contain only basic and summarized data on the inner-core kinematic and thermodynamic characteristics of TCs, they do contain the essential parameters needed for this study. Most notably, they include a consistent and objective determination of eye presence that has remained fairly constant over the past several decades and is unaffected by the limitations of satellite imagery.

Many basic questions remain as to the details of when and where eyes form, the intensities they form at, their observed sizes upon formation, and the environmental characteristics present at the time of eye formation. This paper aims to provide a comprehensive and robust climatology of the formation of the initial TC eye. The problem of secondary eyewall formation is not treated here [see Kossin and Sitkowski (2009) for a climatology of secondary eyewall formation]. The rest of the paper is organized as follows. Section 2 lays out the conditions under which an aircraft eye is reported. Section 3 documents the data used in this study. Section 4 defines the observational stages of eye development that are used as baselines in subsequent data analysis. Section 5 details how cases are selected subject to the availability of aircraft data and the manner in which cases are further stratified for composite analysis. The climatology of eye formation is presented in section 6. A summary and concluding discussion are given in section 7. An online supplement accompanies this article to provide additional supporting materials and background that may be helpful to readers.

2. Definition for the aircraft eye

The keystone of this study is the use of reconnaissance aircraft data to establish whether an eye was present or not. This aircraft-only approach is important because reconnaissance aircraft have used a consistent and reliable method for determining eye presence for the past several decades. Specifically, *an eye is only reported if a circular, precipitating, inner-cloud feature subtends at least half of the candidate eye region* (Weatherford and Gray 1988b) on the aircraft's forward-pointing weather avoidance radar. If the eyewall feature completely encircles the eye region, a *closed eye* is reported. If the eyewall subtends at least 180° of the eye with no breaks, an *open eye* is reported. If the eyewall feature does not encircle at least half the central region, no eye is reported, however the flight meteorologist may include a mention of *partial eyewall* in the remarks. As also described by Weatherford and Gray (1988b), to be considered an eyewall, the circular convective feature must also be distinct from the adjacent spiraling bands. If the convection is not separate from these bands, the descriptor *spiral banding* (or simply *banding*) is often given.

Have differences in radar characteristics lead to differences in eye detection over the years? Probably not. All current U.S. Air Force Reserve (AFRES) WC-130J and the National Oceanic and Atmospheric Administration

TABLE 1. A summary of best track parameters used in this study. The first column gives the symbolic notation used in this study, the second column gives the parameter description, and the third column gives the native units of the parameter in the Best Track dataset.

Best track parameters		
Parameter	Description	Units
BT τ	Date and time of best track point	UTC
BT ϕ	Lat of best track TC center	°N positive
BT λ	Lon of best track TC center	°W positive
BT $p_{\min}$	Best track min sea level pressure	mb
BT $v_{\max}$	Best track 1-min max sustained surface wind speed	kt
b-deck $r_{\max}$	Radius of max winds at the surface from b-deck (not best tracked)	n mi

(NOAA) WP-3D aircraft carry similar 5-cm (C band) weather avoidance radars with comparable operating characteristics (J. Parrish 2009, personal communication). On this radar, which is located in the aircraft nose, the 31-dBZ reflectivity threshold is used to identify eyewall structure because the next lowest threshold (21 dBZ) sometimes includes returns from precipitation aloft or cloud features not part of the eyewall (J. Parrish 2009, personal communication). Flight meteorologists on board the NOAA WP-3D aircraft may also use lower-fuselage radar to determine eye presence. This C-band radar is more powerful, has a larger antenna, and can scan a full 360°, in contrast to the forward-pointing nose rose radar that can only see to the front and sides of the aircraft. Earlier AFRES aircraft used 3-cm (X band) nose radars (Weatherford and Gray 1988b) that were more readily attenuated than the newer C-band nose radars. As a practical matter, the eyewall reflectivities are high enough that the differences between the C- and X-band radars, and nose versus lower-fuselage radars (which can be significant in other contexts), probably do not change the results here. Thus, though this method of determining eye presence is subjective and relies on the judgment of onboard flight meteorologists using various radars over the years, it is more consistent than any other method available.

As described in section 2 of the supplement, compared with remote sensing observations or the full flight level aircraft data, the historical VDM records are more complete, are well suited to studying eye formation, and offer the greatest number of cases. As a result of instrumentation upgrades (see the supplemental material), the last 20 years of Atlantic reconnaissance data are also more accurate than were available to previous studies (Shea and Gray 1973; Gray and Shea 1973; Weatherford and Gray 1988a,b; Kimball and Mulekar 2004; Mundell 1990; Fitzpatrick 1996).

3. Data sources and processing

This study uses several existing datasets, including the Best Track (BT), the Extended Best Track, and the development dataset for the Statistical Hurricane Intensity Prediction Scheme (SHIPS), and develops a new dataset of TC structure parameters from the VDMs. A subjective analysis of infrared satellite imagery provides additional information on the timing of eye formation. This section describes the characteristics of these data and the processing methods used to synthesize the VDM dataset.

a. Best Track dataset

This study uses the National Hurricane Center (NHC) archive best tracks (b-deck files) to establish the best estimates of the TC's position, maximum sustained wind speed, and minimum sea level pressure. All BT data are inherently smoothed in time. As observing technologies have advanced and more platforms have become available, the quality of the BT data has generally improved (McAdie et al. 2009). Over the years, changes in operational practice and knowledge of TC structure (e.g., Franklin et al. 2003) have also led to epochal variations in the quality of the best track TC positions and intensities. Although the b-deck files also contain values for the radius of maximum wind, it is very important to realize that these radii of maximum wind data are *not* best tracked—they are simply the operationally estimated values used for each forecast cycle. The BT parameters used in this study are summarized in Table 1. Additional details are provided in section 4 of the supplement.

b. Extended Best Track dataset

Prior to 2001, NHC's archive best tracks often lack outer wind radii and radius of maximum wind data. To fill in these missing values, this study supplements the b-decks with radius of maximum wind values from the EBT dataset. Like the values for radius of maximum wind in the b-decks, the EBT values for this quantity are obtained from the operational advisories, which are based on operational data sources, including ship and buoy observations, aircraft observations, satellite-derived estimates, and operational analyses. As such, the EBT is a composite dataset derived from sources of varying

TABLE 2. Summary of a subset of the SHIPS environmental parameters. Columns are as in Table 1.

SHIPS environmental parameters		
Parameter	Description	Units
VMPI	Maximum potential intensity (Bister and Emanuel 1998)	kt
RSST	Reynolds SST	°C
E000	1000-mb θ_E (radial average from 200 to 800 km)	K
D200	200-mb divergence (radial average from 0 to 1000 km)	10^{-7} s^{-1}
T200	200-mb temperature (radial average from 200 to 800 km)	°C
SHDC	850–200-mb shear magnitude with vortex removed (radial average from 0 to 500 km)	kt
VVAV	Avg (0–15 km) vertical velocity of a parcel lifted from the surface accounting for entrainment, ice phase, and condensate weight (radial average from 200 to 800 km)	m s^{-1}

quality, so the additional EBT size parameters have generally *not* benefited from any postseason analysis (Demuth et al. 2006). In most cases, the radii were simply copied from the a-decks (files that contain operational guidance) to the b-decks by the Automated Tropical Cyclone Forecast (ATCF) system (Sampson and Schrader 2000; B. Sampson 2010, personal communication). We have uncovered inconsistencies in the EBT's radius of maximum wind values for a number of TCs in the early period of that dataset. Prior to 2001, plots (not shown, see appendix E of Vigh 2010) show many cases of poor correspondence between the EBT radii of maximum winds and actual aircraft measurements.

The EBT dataset also contains an estimate of eye diameter and could therefore have been used to determine eye presence as was done in Kimball and Mulekar (2004). However, the EBT eye diameters are provided both when the TC was observed by aircraft and when it was observed only by satellite. As a result, the EBT determinations of the presence of an eye and its diameter are not consistent throughout that dataset.

c. SHIPS developmental dataset

Since the statistical-dynamical SHIPS intensity forecast aid incorporates a wide array of environmental, satellite, and model-based parameters to make skillful predictions of TC intensity (DeMaria and Kaplan 1994, 1999; DeMaria et al. 2005), the developmental dataset on which its predictor relationships are developed provides a convenient way to access information about the changing environmental conditions for past TCs. The SHIPS dataset covers all named TCs in the Atlantic and eastern Pacific basins from 1982 onward; starting in 1989, it also includes unnamed Atlantic tropical depressions. For 1982–2000, the predictors were derived from the National Centers for Environmental Prediction (NCEP) reanalysis fields. From 2001 onward, the predictors have been obtained from the operational analyses and forecasts of the real-time runs of the Global Forecast System (GFS) model. Approximately 50 predictors are available from 0 to 120 h at 6-h intervals relative to the time and date of each case. This study only uses a small subset of these predictors to ascertain the favorableness of the TC environment at the analysis time of the operational model ($t = 0$ h); no model forecasts are used here. Table 2 summarizes the SHIPS parameters used.

d. CIRA GOES IR satellite archive

To provide a comprehensive cloud-top view of the TC during eye formation, we use IR satellite imagery generated from the Cooperative Institute for Research in the Atmosphere (CIRA) Geostationary Operational Environmental Satellite (GOES) IR satellite archive (IR archive hereafter). That archive spans 212 Atlantic TCs from 1995 to the present and consists of digital brightness temperatures from the IR channel 4 (10.7 μm) in a window centered on the moving TC center (Zehr and Knaff 2007). From these brightness temperature data, images were generated at 15- or 30-min intervals and subjectively analyzed according to criteria described in section 4.

e. VDM dataset

The VDMs contain a wealth of information about TC intensity and structure. Each VDM contains data associated with a single vortex fix made by the aircraft. Once the fix center has been determined, a VDM is created and transmitted back to the Chief, Aerial Reconnaissance Coordination, All Hurricanes (CARCAH) at NHC in near–real time to provide the operational forecasters with rapidly updated information on the TC. An example VDM from Hurricane Rita (2005) is provided in Fig. 1. This VDM, taken on the 700-mb flight level when Rita was near peak intensity, indicates a maximum flight level temperature in the eye of 31°C. Since the dewpoint at that location was −3°C, the resulting dewpoint depression was 34°C. To the authors' knowledge, this is the highest eye temperature, the lowest dewpoint temperature, and the greatest dewpoint depression ever measured in a TC at the 700-mb flight level.

From 1989 to 2008, reconnaissance aircraft made a total of at least 4954 unique vortex fixes in 205 TCs in the

```
URNT12 KNHC 220739
VORTEX DATA MESSAGE
A. 22/07:14:30Z
B. 24 deg 48 min N
   087 deg 46 min W
C. 700 mb 2208 m
D. NA  kt
E. NA  deg     nm
F. 225 deg 148 kt
G. 134 deg 013 nm
H.         899 mb
I.   9 C/ 3047 m
J.  31 C/ 3043 m
K.  -3 C/ NA
L. CLOSED WALL
M. C16
N. 12345/ 7
O. 0.02 / 1  nm
P. AF307 1618A RITA          OB 11
MAX FL WIND 165 KT NE QUAD 05:34:00 Z
STADIUM EFFECT VERY VISIBLE IN MOONLIGHT
FREQUENT LIGHTNING WITHIN EYEWALL
```

FIG. 1. Example VDM from Hurricane Rita for the vortex fix taken at 0714 UTC 22 Sep 2005. For further explanation of the VDM format and contents (see section 5 of the supplement).

Atlantic, eastern Pacific, and central Pacific basins. Since TCs in the eastern and central Pacific basins do not often threaten land, they are not normally reconnoitered frequently enough to be of use for this study. Thus, the remainder of this study focuses on the 4692 VDMs taken from the 183 TCs that occurred in the Atlantic basin during this period.

Each VDM has been decoded and translated into parameters describing the structure and intensity of the TC. Table 3 summarizes the parameters obtained directly from the VDMs. For more details on the VDM format and how the VDM parameters have been decoded and translated, the reader is referred to section 5 of the supplement (Table S2 in the supplement provides an expanded version of Table 3 that includes additional derived dynamical quantities). The parameters of the combined dataset utilize a combination of nautical units [knots (kt), nautical miles (n mi), millibars (mb)] and SI units. The native units of each source dataset are preserved in this study to allow for the most effective quality control of these data and to provide results in units that are familiar to the operational forecasting community (1 kt = 0.5144 m s^{-1}, 1 n mi = 1.852 km, 1 mb = 1 hPa, and °C = kelvins −273.15).

A summary table (Table S3 in the supplement) provides a catalog of all 205 TCs that were observed by aircraft reconnaissance in the Atlantic, eastern Pacific, and central Pacific basins from 1989 to 2008. From the 4924 unique VDMs, this table characterizes the observed ranges of kinematic and thermodynamic parameters over each TC's lifetime.

4. Determination of eye development baselines

With the VDM data translated, the next task is to define meaningful and robust definitions for discrete, observable stages of eye development. From both a forecasting perspective, and the perspective of the dynamical evolution of a TC, it must be kept in mind that eye formation is a process, not an event. Nevertheless, to achieve the aims of this study it is necessary to determine the initial point in time that each eye development stage was observed in a given TC. We will refer to these discrete stages as *eye development baselines*. Likewise, we will refer to the time when a TC was first observed to manifest these initial eye or pre-eye characteristics as *baseline times*. Once these baseline times have been determined, we then apply selection criteria to all eye-forming TCs to identify which TCs should be included as cases.

a. Eye development baselines observed by aircraft

Following the principles outlined in section 2, an *aircraft eye* is considered to be present if *either* of the following conditions are met:

- The VDM eyewall completeness descriptor contains the words "open" or "closed," or
- the aircraft reports an eye diameter descriptor *and* the eyewall completeness descriptor contains one of the following: "poor," "weak," or "ragged."

Sometimes the eyewall completeness descriptors are unclear, so we make several assumptions in treating these. We consider the descriptors "broken," "breaks," and "semi circle" to be synonymous with an open eyewall and map these accordingly in the dataset. The eyewall definition descriptors poor, weak, and ragged are indeterminate without additional information, so as long as the eye was defined well enough that air crews were able to report an eye diameter, we assume that these eyewall descriptors correspond to valid open eyes. If the eye was reported to be poorly defined but no diameter was given, we designate it as a "poorly defined eye." Finally, air crews sometimes reported spiral banding for several fixes before a bona fide eye appears; in the dataset, we store such values separately from eye presence.

TABLE 3. Summary of parameters obtained from the VDMs. The first column provides the symbolic notation used in the remainder of this study. The second column contains descriptions of each parameter. The third column gives the corresponding section of the VDM that this parameter is obtained from (section names use the original phonetic alphabet). The last column gives the native units of the parameter in the VDM dataset. The shorthand notation "FL" indicates that the observation pertains to flight level.

Directly-obtained VDM parameters			
Parameter	Description	VDM section	Units
VDM τ	Date and time of the vortex fix	ALPHA	UTC
VDM ϕ	Lat of the fixed surface center	BRAVO	°N
VDM λ	Lon of the fixed surface center	BRAVO	°W
FL SAS	Standard atmospheric surface of flight level for current fix	CHARLIE	mb or ft
FL $H_{\min}$	Min height of the flight level SAS observed inside the center	CHARLIE	m
Surface $v_{\max,\text{in}}$	Max surface wind speed observed during the inbound leg of current fix	DELTA	kt
Surface $r_{\max}$	Radius of max surface winds (range of surface $v_{\max,\text{in}}$ from center fix coordinates)	ECHO	n mi
Surface $v_{\max,\text{out}}$	Max surface wind speed observed during the outbound leg of current fix	Remarks	kt
Surface $V_{\max}$	Combined max surface wind speed (see the supplement for details)	DELTA or remarks	kt
FL $v_{\max,\text{in}}$	Max flight level wind speed observed during the inbound leg of current fix	FOXTROT	kt
FL $r_{\max}$	Radius of max flight level winds (range of flight level $v_{\max,\text{in}}$ from center fix coordinates)	GOLF	n mi
FL $v_{\max,\text{out}}$	Max flight level wind speed from outbound leg of current fix	Remarks	kt
FL $v_{\max}$	Combined max flight level wind speed (see the supplement for details)	FOXTROT or Remarks	kt
VDM $p_{\min}$	Min sea level pressure (obtained by extrapolation or dropsonde)	HOTEL	mb
T_{out}	Max flight level temperature observed just outside the eyewall or max wind band	INDIA	°C
T_{eye}	Max flight level temperature observed within 5 n mi (9.3 km) of center fix coordinates	JULIET	°C
T_{sup}	Supplementary max flight level temperature observed more than 5 n mi (9.3 km) from center fix coordinates	Remarks	°C
$T_{d,\text{eye}}$	Dewpoint temperature observed at same location as T_{eye}	KILO	°C
d_{eye}	Diameter of primary eye	MIKE	n mi

Once the eye presence (or nonpresence) has been determined for each VDM fix, the data for each TC are objectively screened to determine the first time that an aircraft observed each of the following stages of eye development:

1) **First spiral banding (B):** The time of the first fix that contains the words "bands," "banding," or "spiral."
2) **First open aircraft eye (A1):** The time of the first fix for which reconnaissance aircraft reports an open radar eye.
3) **First closed aircraft eye (A2):** The time of the first fix for which reconnaissance aircraft reports a closed radar eye.
4) **First aircraft eye (A):** The time of the first fix for which reconnaissance aircraft reports any radar eye (whether open or closed).

b. *Eye development baselines observed by satellite*

To determine when the IR *eye* formed, we subjectively analyzed the brightness temperatures ($T_{b,\text{IR}}$) from the IR archive to obtain the first date/time that the TC reached each of the following stages of eye development:

1) **First open warm spot (IR1):** The time of the IR satellite image when an open warm spot first appears near the TC center. The warm spot may be manifested as a region of warm $T_{b,\text{IR}}$ embedded in a cold cloud shield, or as a larger, central clear area of warm $T_{b,\text{IR}}$ encompassed by surrounding deep convection. In either case, the warm spot must be at least two-thirds surrounded by cloud tops of colder $T_{b,\text{IR}}$.
2) **First closed warm spot (IR2):** The time of the IR satellite image when a closed warm spot first appears near the TC center. Colder cloud tops must completely surround the warm spot.
3) **First eye (IR3):** The time of the IR satellite image when the warmest $T_{b,\text{IR}}$ of the closed warm spot first exceeds −50°C *or* is at least 15°C warmer than nearby cloud tops of the surrounding convection. Every point on the surrounding ring of coldest $T_{b,\text{IR}}$ must be less than the $T_{b,\text{IR}}$ of the warm spot.
4) **First persistent eye (IR4):** The beginning point of the time period when the TC first maintains an eye (according to the criterion of IR3) for at least 6 h.
5) **First strong eye (IR5):** The first time that the warmest eye $T_{b,\text{IR}}$ exceeds −30°C and is at least three-quarters surrounded by a ring of cold cloud tops with $T_{b,\text{IR}}$ colder than −70°C. In general, the eye should be fairly symmetric to be considered a strong eye.

Because of the transient nature of convection, our subjective classification is somewhat uncertain for the IR1, IR2, and IR3 stages. The degree of subjectivity decreases from IR1 to IR5, however. Compared with IR3, the IR4 stage provides a more robust classification because the eye must persist for a testing period (6 h). In some cases, the eye became ill defined after first appearing and did not meet the precise definition of an eye for an image or two. As long as the eye generally persisted and remained at the end of the 6-h period, we have classified the case as a persistent eye (IR4). For the IR5 stage, insufficient resolution or an oblique viewing angle may prevent the eye's true maximum $T_{b,\mathrm{IR}}$ from being observed. These factors may critically affect whether or not a strong eye classification is made, especially for TCs with tiny eyes. As an example, Hurricane Opal (1995) was never classified as attaining IR5 because its pinhole eye[1] did not display a pixel warmer than −30°C.

c. Record of eye development baseline times

Using the above criteria, we recorded the date and time that each aircraft or satellite eye development baseline was reached for each TC (see Table S4 in the supplement).

5. Selection of cases

With the initial eye formation times determined, the next task is to determine which eye formation events were sufficiently observed by aircraft to be included as cases in this climatology. Here we choose to focus entirely on the initial eye development in each TC's life cycle; all subsequent reformations are neglected. This choice makes our results as applicable as possible to forecasters tasked with predicting TCs that have not yet formed eyes. Thus, each eye-forming TC can only be included as one case in this study.

Eye formation can be a rather ephemeral process and the irregular aircraft sampling can make classification of cases a challenge. To select cases as objectively as possible, we require that valid cases satisfy the following dual criteria: at least one aircraft fix must have been taken *prior* to the first aircraft fix that reports an eye, and the time interval between the prior eyeless fix and the first eye fix cannot exceed 12 h. These criteria ensure that an eye was not already present by the time aircraft observations had commenced and that cases are excluded if the eye could have formed a considerable length of time before the fix in which it was first observed. This guideline is a compromise between including as many cases as possible and minimizing the uncertainty as to when the eye formed. In fact, the average length of time between the eye-forming fix and the previous fix (4.2 h, with a standard deviation of 2.9 h) is much less than 12 h.

a. Stratification of cases

To further stratify the eye formations, cases are objectively classified according to the duration and persistence of the initial eye (or subsequently reformed eyes) during the 72-h period following the first eye report by aircraft. We impose this 3-day window to avoid considering cases in which an eye reforms many days later in a completely different environment. Our categories are described as follows (the number of TCs in each case type is shown in parentheses):

1) **No aircraft data [127 (87 of these were after 1994)]:** 1 or fewer aircraft fixes were taken (none in most cases).
2) **No observed eye [76 (66 of these were after 1994)]:** No aircraft eye was reported in the TC during the period of aircraft observations (although it is possible that an eye could have formed at some other time).
3) **Insufficient data (9):** An eye was reported by aircraft for at least part of the TC's lifetime, but the timing of the eye formation cannot be determined because the eye formed after aircraft observations ceased or because the aircraft fixes were too infrequent to determine the time of formation to within 12 h.
4) **Eye already present (28):** The initial eye formed before the period of aircraft observations began.
5) **Rapid dissipation (17):** The initial aircraft eye was reported for a period of less than 24 h and then dissipated without any further aircraft observations of eye reformation.
6) **Intermittent formation (24):** The sequence of aircraft fixes indicates that the initial eye had dissipated and subsequently reformed (possibly multiple times) without any of these eyes lasting longer than 24 h. Such a sequence includes one or more fixes with an aircraft eye (the initial eye), followed by at least one eyeless fix, followed by one or more additional aircraft eye reports.
7) **Delayed formation (12):** The initial aircraft eye formed and then dissipated, or was intermittent for a time, but then eventually lasted for at least 24 h without subsequent interruption.

[1] Pinhole eyes are very small eyes that are not well resolved by GOES IR satellite imagery (spatial resolution of approximately 4 km), but that can be seen in higher-resolution channels such as visible imagery (Olander and Velden 2007).

8) **Sustained formation (17):** The initial aircraft eye formed and was sustained for at least 24 h without interruption.

With all TCs classified according to the duration and persistence of their initial eye formations, the methodological foundation has been laid for the climatology.

b. Representativeness of cases

The vast majority of Atlantic TCs (240 of 310, or 77%) fall into the first four case types (no aircraft data, no observed eye, insufficient data, and eye already present). Since the time of eye formation cannot be determined for these cases, they are unusable for the purposes of this study. Given the limited geographic range and intermittent nature of aircraft reconnaissance flights, it is useful to consider how the vagaries of aircraft sampling affect the selection of cases. Do the remaining eye-forming cases provide a sample that is representative of the broader set of Atlantic TCs? To answer this question, we analyzed the spatial and temporal characteristics of the other case types as well as the median value of the distributions of each case type for TC longevity, intensity, structure, and environmental parameters (see Figs. S1–S5 and Table S1 in the supplement). Highlights of this analysis are discussed in the next paragraph; for more details, readers are referred to section S6 of the supplement.

Generally, the TCs in the ''no aircraft data'' case type tracked through the central and eastern Atlantic well beyond the range of aircraft. A smaller subset of TCs in this group formed very close to land and then quickly made landfall (e.g., the southern Bay of Campeche), while yet another subset include a number of TCs that tracked through the central Atlantic and higher latitudes. The recurving tracks of the east Atlantic TCs, along with the fact that satellite eyes were observed in many of them, point to the idea that many of these cases were Cape Verde hurricanes that simply recurved well before threatening land. In contrast, the ''no observed eye'' cases were constrained to be within the domain of aircraft reconnaissance by definition. Many of these TCs originated in the Gulf of Mexico and had both short tracks and short lifetimes (a median longevity of just 54 h). Another cluster of eyeless TCs formed in the eastern portion of the basin, but then dissipated near the Caribbean, probably due to adverse environmental vertical wind shear [the median wind shear for this case type is 18 kt (9.4 m s^{-1}), the highest of all the case types]. Not surprisingly, the TCs in this case type have the lowest median intensity and are found predominantly at higher latitudes and more western longitudes than any of the other case types. The ''insufficient data'' case type contained too few cases to make any generalizations. The tracks of the ''eye already present'' cases are strongly indicative of Cape Verde hurricanes that underwent genesis and formed eyes well east of the domain of aircraft reconnaissance. The median intensity of these cases is much higher [79 kt (40.6 m s^{-1})], and the median minimum central pressure is much lower (971.5 mb), than any of the other case types. These TCs also lasted much longer (261 h) than even the sustained formation cases (210 h). In summary, while the geographic constraints of aircraft reconnaissance limit the numbers of Cape Verde hurricanes, higher-latitude TCs in the central Atlantic, and short-fuse tropical storms in and near the Gulf of Mexico, the remaining sample includes ample numbers of similar systems, so we find no compelling evidence to suggest that this aircraft-only sample is not representative of the broader set of TCs that form eyes in the Atlantic basin. The impact of case selection using only aircraft data probably biases our sample toward TCs that formed eyes over somewhat higher SSTs. Our sample may also be slightly biased toward shorter-lived TCs, owing to the greater preponderance of landmasses in the western half of the basin. Nevertheless, the next section shows that the remaining eye-forming cases share many characteristics in common with the broader set of TCs.

6. Results

This section presents a comprehensive climatology of hurricane eye formation. Of the 310 Atlantic TCs that occurred from 1989 to 2008, 183 have sufficient data (at least two center fixes) to be included in the VDM dataset. Of these, 70 TCs formed eyes and were sufficiently observed by aircraft data to be selected as cases. The IR archive covers a shorter period from 1995 to 2008 and contains 193 TCs with sufficient satellite coverage. From these data, we compute the frequency of eye formation and then determine the geographic origin of TCs and their distribution in the season. Next we examine the basic statistics at the time when aircraft first reported an eye. The environmental conditions under which eyes form are summarized. Eye formation cases are then analyzed throughout the TC life cycle to determine where and when eye formations occur. With these results in hand, we seek to address some remaining questions such as the time scale for eye formation.

a. Frequency of eye formation

How frequently do eyes form? Table 4 shows the number of TCs and the associated frequencies of occurrence for each stage of eye development. All frequencies are computed using the above sample sizes (i.e.,

TABLE 4. Frequency of eye formation by development stage for Atlantic TCs. First group: Aircraft-observed TCs displaying banding. Middle group: Aircraft-observed TCs for which an eye was reported. Last group: Stages of eye development obtained from subjective classification of IR satellite images. Frequencies for aircraft observables are computed using a base of 183 TCs that had at least two fixes. Frequencies for satellite observables are computed using a base of 193 TCs that had sufficient IR satellite coverage.

Frequency of eye formation			
Code	Observational baseline	No. of TCs	
	Aircraft observations of banding		
B1	Banding, no aircraft eye	16	8.7%
B2	Banding, aircraft eye observed at any point	62	33.8%
B3	Banding observed prior to aircraft eye	40	21.9%
B	Any banding (B1 ∪ B2)	78	42.6%
	Aircraft observations of eyes		
PD	Poorly defined aircraft eye	3	1.6%
A1	Open aircraft eye	104	56.8%
A2	Closed aircraft eye	84	45.9%
A	Any aircraft eye (PD ∪ A1 ∪ A2)	107	58.5%
	IR satellite observations of eyes		
IR1	Open warm spot	176	91.2%
IR2	Closed warm spot	147	76.2%
IR3	Eye	118	61.1%
IR4	Persistent eye	82	42.5%
IR5	Strong eye	41	21.2%

183 for aircraft and 193 for IR satellite imagery). Since we seek to estimate the true frequency of eye formations in the full population of Atlantic TCs, all aircraft data are included whether or not the TC was regarded as being under aircraft observation at the time of eye formation (i.e., insufficient data cases are included in these frequency computations).

Banding is often noted by aircraft prior to observation of the actual aircraft eye. In fact, aircraft-observed banding occurred at some point in the lifetimes of 78 of the 183 aircraft-observed TCs (43% of all TCs). Of the 78 TCs that displayed banding, 16 never formed eyes (21% of TCs with banding). Of the remaining 62 TCs that did form eyes, the first observation of banding sometimes occurred *after* the eye had already formed and/or dissipated. In just over half the banded TCs (40 TCs, 51%), the first report of banding preceded the first report of an aircraft eye, so banding can indicate that an eye is in the process of forming. However, since banding is not always reported before the eye forms, its usefulness to forecasters may be somewhat limited.

An aircraft eye (A, open, closed, or poorly defined) was reported in 107 (58.4%) of the 183 systems. Because of the potential undersampling of the VDM data, this percentage may slightly underestimate the true frequency. The more consistent temporal sampling of the geostationary satellite platform yields a different frequency for *satellite* eye observation that applies to the broader population of Atlantic TCs. An IR satellite eye (IR3) was observed in 118 (61.1%) of all systems with sufficient satellite coverage. Just 82 (42.5%) of IR-observed systems satisfied the more stringent requirements for a persistent eye (IR4) however. Given the uncertainties in the IR3 classification, it is possible that the IR3 proportion somewhat overestimates the true frequency of eye formation.

During the study period, 126 TCs were observed by both aircraft and IR satellite imagery; this allows for a homogeneous comparison of observations from the two platforms. Of these dually observed TCs, an aircraft eye was reported in 73 TCs (57.9%), while a satellite eye (IR3) was reported in 86 TCs (68.3%). An eye was observed by both aircraft and IR satellite imagery in 69 TCs (54.8%). Accounting for the potential overestimation of the IR3 classification and the undersampling of aircraft observations, we estimate that the true frequency of eye formation for all TCs in the basin is about 60%. For comparison, 101 (52.3%) of the satellite-observed TCs became hurricanes.

The results for the remainder of this study exclude TCs that never possessed an aircraft-observed eye (the 73 no observed eye cases) and TCs for which aircraft data were insufficient to determine the time of eye formation (the 37 insufficient data cases). This leaves 70 data-rich eye-forming TCs out of the 183 aircraft-observed TCs that were available.

b. Geographic origin and seasonal distribution

Where do the eye-forming TCs come from? Figure 2 shows the origin of each eye-forming TC, taken to be the first best track point. Cases are stratified by the duration and persistence of the eye formation events. Most

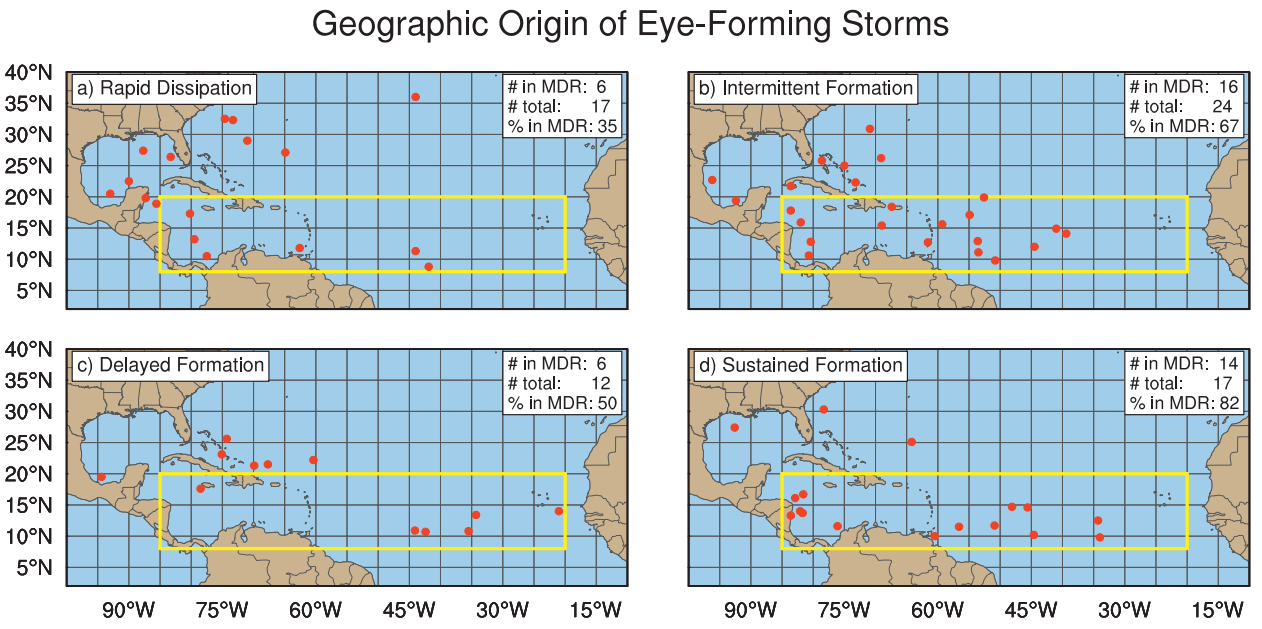

FIG. 2. Geographic origin of the 70 eye-forming cases. The origin of the TC is taken to be the first best track point (red dots). The modified MDR (a box bounded by 8°–20°N, 20°–85°W) is indicated by the yellow box. Results are shown for the following case types: (a) rapid dissipation, (b) intermittent formation, (c) delayed formation, and (d) sustained formation.

TCs that later become major hurricanes [maximum sustained surface winds of at least 100 kt (51 m s^{-1})] form in association with African easterly waves (AEWs). Most of these TCs develop in an area of the deep tropical Atlantic known as the main development region (MDR; Goldenberg et al. 2001). Of the rapid dissipation cases (Fig. 2a), only 35% have their origin in the MDR. Many rapid dissipation cases originated at higher latitudes or in the Gulf of Mexico which is typical of TCs forming in the early or late season. In contrast, 67% of the intermittent formation cases (Fig. 2b) originated within the MDR. These intermittent formation TCs likely originated from AEWs but then encountered detrimental environmental conditions. Meanwhile, 50% of the delayed formation cases (Fig. 2c) came from the MDR, but fully 82% of the sustained formation cases (Fig. 2d) originated in the MDR.

Taken together, these data suggest that TC origin has a significant influence on whether or not the system can form a lasting eye. We speculate that the geographic origin of a TC is closely related to the environment it subsequently experiences. If true, then TCs that form from AEWs in the deep tropics tend to encounter favorable environments, while TCs that form from subtropical influences tend to have marginal environments. More can be learned by considering when eye formations occur during the season.

Figure 3 shows the monthly distribution of TCs that formed eyes compared with the monthly distribution of TCs that reached minimal hurricane intensity. In this sample, eye formations are relatively frequent during the months of July, August, September, and October; eyes formed much less frequently during the month of November, and no aircraft eyes were observed during the months from December to June. This is not to say that eyes cannot form during those months, but merely that eye formations are relatively infrequent. When they do happen, they tend not to be observed by aircraft.

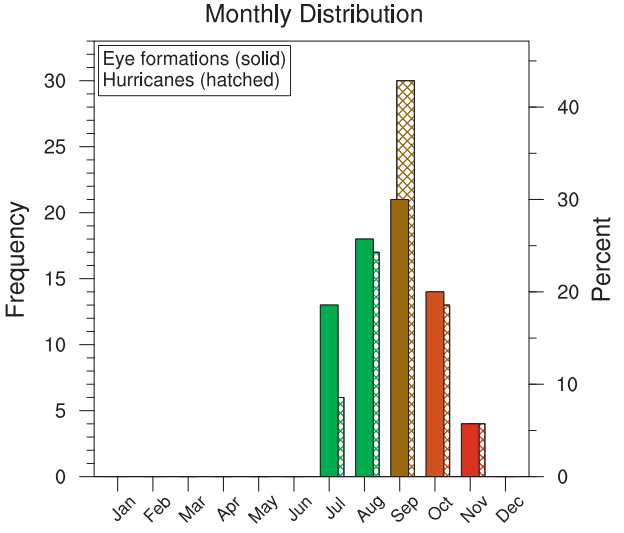

FIG. 3. Monthly distribution of eye formations (solid) and TCs that became hurricanes (hatched) for the 70 eye-forming cases in this study.

TABLE 5. Summary of basic statistics at the time of first aircraft eye report for the 70 Atlantic TCs that were well observed during their eye formation periods, 1989–2008. BT quantities have been interpolated to the time of aircraft eye formation. Columns are as follows: number of fixes taken during the each TC's lifetime; best track minimum central pressure (BT p_{min}); minimum central pressure from extrapolation or dropsonde (VDM p_{min}); 6-hourly translation speed of the TC computed from best track positions; latitude of fix (VDM ϕ); longitude of fix (VDM λ); best track surface wind speed (BT v_{max}); range of maximum flight level wind (FL r_{max}); and diameter of initial eye (VDM d_{eye}).

	No. of fixes	BT p_{min} (mb)	VDM p_{min} (mb)	TC translation speed (m s^{-1})	VDM ϕ (°N)	VDM λ (°W)	BT v_{max} (kt)	FL r_{max} (n mi)	VDM d_{eye} (n mi)
				Measures of central tendency					
Mean	37.0	990.8	992.2	4.52	22.28	76.04	58.1	25.0	18.7
Median	33.0	991.0	992.0	4.43	21.61	76.61	58.0	18.5	18.0
				Measures of spread					
Std dev	21.0	7.8	8.0	2.43	6.08	11.72	11.9	20.3	9.8
IQR	29	9	10	3.3	9.6	19.5	16	19	15
				Measure of symmetry					
Yule–Kendall	0.0	−0.1	0.0	−0.19	0.10	−0.24	0.0	0.2	−0.1
				Additional measures					
No. of records	70	69	70	70	70	70	70	70	69
Max	96	1009	1007	10.6	37.3	96.7	88	105	45
75%	48	995	997	5.8	26.9	84.1	66	30	25
25%	19	986	987	2.5	17.3	64.5	50	11	10
Min	8	968	969	0.1	12.3	56.5	29	2	2

Curiously, the monthly distribution of eye formations differs markedly from the distribution of hurricanes during the months of July and September. In July, more TCs form eyes than become hurricanes, while in September, considerably more TCs become hurricanes than form eyes. July's eye formation cases experience rapid dissipation at a higher rate (31%) than the other months (21%–25%). Our previous analysis of the geographic origin of cases shows that many of these July cases form in and near the Gulf of Mexico and then make landfall. Meanwhile, September's eyeless hurricanes might be explained by the fact that that month features the most favorable environmental conditions for genesis and intensification. For whatever reason, a significant number of September TCs are disrupted to the point that they cannot form eyes.

c. Basic statistics at time of eye formation

The data offer answers to a number of basic questions: At what intensities and minimum central pressures do eyes form at? How fast are TCs moving when they form eyes? How large are the eyes when they form? Table 5 provides a statistical summary of several parameters at the time of the first report of an aircraft eye (for values at each individual eye formation event, see Table S5 in the supplement). The number of fixes taken over a TC's lifetime (second column of Table 5) can be taken as a rough measure for how well TCs were sampled. In our sample, this number ranges from 8 to 96 fixes. The median of 37 fixes means that most TCs were sampled many times per day, so we have confidence that most of our cases were well observed.

1) MINIMUM CENTRAL PRESSURE, P_{MIN}

For comparison, we present minimum central pressure statistics at the time of eye formation for both BT p_{min} (interpolated to the time of the first aircraft eye) and the directly observed VDM p_{min}. For the 70 cases in our climatology, the medians are essentially the same: 991 and 992 mb. We take the first and third quartiles (25% and 75% percentiles) to represent the range of typical values. (These values contain the central 50% of values.) Thus, most eyes form at minimum central pressures between 997 and 987 mb.

2) LATITUDE AND LONGITUDE

All TCs in the sample formed eyes between 12.3° and 37.3°N. More typically, eyes formed within a narrower range of 17.3°–26.9°N. Eyes formed across a wide longitudinal range delimited by the western edge of the basin boundary (96.7°W) and the eastern cutoff of routine aircraft reconnaissance (56.5°W). The median longitude of eye formation is 76.6°W.

3) TRANSLATION SPEED, C

Eyes form over a wide band of translation speeds, ranging from nearly stationary to over 10 m s^{-1}. The median translation speed is 4.4 m s^{-1} with a typical range of 2.5–5.8 m s^{-1}. Given that high translation speeds cause large and asymmetric boundary layer forcing to the vortex (Shapiro 1983), we are not surprised to find an upper

limit on the translation speeds at which eyes can form. This result is consistent with Knaff et al. (2010), who found that relatively few (<10%) TCs with $v_{max} > 77$ kt (40 m s^{-1}) travel faster than 14 kt (7.2 m s^{-1}; see their Table 1).

4) Maximum sustained surface wind speed, BT v_{MAX}

What intensities do eyes form at? The median interpolated BT v_{max} value is 58 kt (30 m s^{-1}), with a typical range of 50–66 kt (26–34 m s^{-1}). The minimum intensity at which an aircraft eye was observed to form was 29 kt (15 m s^{-1}). The maximum observed intensity at eye formation was 88 kt (45 m s^{-1}). Clearly, eyes form throughout a large range of intensities. *In general, the aircraft eye often forms at a lower intensity than the threshold for hurricane strength.*[2]

5) Radius of maximum wind, R_{MAX}

For the purposes of this study, we take r_{max} to be the distance from the vortex's surface center out to the radial location of the flight level $v_{max,in}$. Since the eyewall typically slopes outward with height, this FL r_{max} is typically found at a somewhat larger radius than the surface r_{max} (Jorgensen1984a,b; Powell et al. 2009; Stern and Nolan 2011). Taking just the data from the fixes at which the aircraft eye was first observed, we find that the median r_{max} is 18.5 n mi (34 km). The mean r_{max} [25 n mi (46 km)] is considerably higher than the median r_{max} because the distribution is skewed toward larger radii by outliers. At the time of eye formation, r_{max} typically ranges from 11 to 30 n mi (20–56 km); however, eyes have been observed to form both at very small r_{max} [as low as 2 n mi (3.7 km)], and at very large r_{max} [up to 105 n mi (195 km)].[3]

6) Eye diameter, d_{EYE}

The newly formed eyes typically have *diameters* at flight level (d_{eye}) that are comparable to the *radii* of maximum winds. The median d_{eye} at formation is found to be 18 n mi (33 km), which means that the median eye *radius* of 9 n mi (16 km) is roughly half the median r_{max} of 18.5 n mi (34 km) at the time of formation.

Compared to the typical range of r_{max} at the time of eye formation, the typical range of d_{eye} is truncated on the upper end: 75% of eyes form at diameters of less than 25 n mi (46 km). The largest diameter of a newly formed eye was just 45 n mi (83 km), which is considerably smaller than the largest r_{max} of 105 n mi (195 km). These results suggest that eyes are normally small to moderate sized when they form. TCs rarely form large eyes initially and apparently, very large eyes never form.

d. Variation of parameters for all eye development baselines

To ensure that our eye development baselines are meaningful, it is instructive to consider the degree of variation across the nine eye development baselines for the medians of several parameters. Table 6 presents median values for several parameters for the aircraft (B, A, A1, and A2) and satellite baselines (IR1 through IR5). For comparison, the medians over the entire lifetimes of all 70 TCs in the sample are presented in the final column.

For the median latitudes and longitudes, the medians of the eye development baselines lie farther south and west than the medians taken over all TC lifetimes. This result likely reflects the simple fact that TCs normally develop as they move along typical tracks toward the west and northwest from their genesis location.

The medians of translation speed exhibit little systematic variation across all eye development baselines, except that the medians of all eye development baselines are slower than the median taken over all TC lifetimes.

The medians of minimum central pressure (p_{min}) progress strongly from higher to lower pressures as TCs develop better defined eyes. This is especially true for the satellite baselines: the median BT p_{min} varies from 1004 mb for the first open warm spot (IR1) down to 963 mb for strong eyes (IR5). For comparison, the median p_{min} taken over all TC lifetimes is just 996 mb.

For intensity, the medians of BT v_{max} show a strong progression from lower to higher intensities as eyes form and become better defined. This increases confidence that our eye development baselines are meaningful indicators.

The medians of FL r_{max} show a strong progression from larger to smaller radii as the eye develops. Most notably, r_{max} undergoes a significant contraction from the pre-eye development baselines to the time when the eye is initially observed. For example, from the time the aircraft first observes banding (B) to the time that it first observes an open eye (A1), the median r_{max} contracts from 31 n mi (57 km) down to 20 n mi (37 km).

[2] The astute reader may now recognize that the title of this paper is somewhat misleading.

[3] Note that the aircraft-based r_{max} measurements often fluctuate rapidly in time. This scatter arises due to several factors: 1) TCs do not always possess a sharp peak in tangential wind and 2) aircraft sample specific azimuths through TCs that are often asymmetric. Because of these factors, the r_{max} statistics taken from the fix of the first reported eye probably overstate r_{max} somewhat. A more robust estimate of r_{max} at the time of eye formation could be obtained by interpolating the time-trended lower bound of observed r_{max} values to the time of eye formation. While such an analysis is beyond the scope of the present paper, we plan to present a refined estimate for r_{max} at the time of eye formation in a follow-up paper.

TABLE 6. Summary of median values for the 9 eye development baselines for the 70 Atlantic TCs that were well observed during their eye formation periods, 1989–2008. Latitude of fix (BT ϕ), longitude of fix (BT λ), TC translation speed computed from BT positions (BT C), BT minimum central pressure (BT p_{min}), BT surface wind speed (BT v_{max}, interpolated), range of maximum flight level wind (FL r_{max}), and diameter of initial eye (VDM d_{eye}). For comparison, median values for these parameters are also given for the entire lifetime of the eye-forming TCs in the sample (last column).

		Median values									
		Aircraft baselines				Satellite baselines					Over TC
Parameter	Units	B	A	A1	A2	IR1	IR2	IR3	IR4	IR5	lifetimes
BT ϕ	°N	21.1	21.6	22.8	22.7	16.9	17.4	19.4	22.6	20.4	25.4
BT λ	°W	77.8	76.6	75.6	77.0	75.1	77.9	76.4	78.0	78.1	73.1
BT C	m s^{-1}	3.6	4.4	4.4	4.8	4.3	4.1	4.8	4.4	4.0	5.1
BT p_{min}	mb	999.0	991.0	992.0	986.5	1004.0	998.5	989.0	975.5	963.5	996.0
BT v_{max}	kt	50.0	58.0	55.5	66.0	34.0	44.0	62.5	79.0	96.0	50.0
FL r_{max}	n mi	31.0	17.5	20.0	17.0	44.0	26.4	21.9	20.1	14.0	26.0
VDM d_{eye}	n mi		18.0	18.0	20.0			26.1	24.3	22.3	20.0

Similarly, from the time an open warm spot (IR1) is first observed on satellite imagery to the time that the TC displays the first satellite eye (IR3), r_{max} contracts from 44 n mi (81 km) down to 22 n mi (41 km). This contraction of the eye is consistent with the theoretical and observational literature on eyewall dynamics from the early 1980s (Smith 1981; Shapiro and Willoughby 1982; Schubert and Hack 1982).

Once the eye forms, both the median r_{max} and the median eye diameters settle into a narrow range with just a slow decrease even as the eye reaches greater definition (A, A1, A2, and IR3 and IR4). The physical scale of the inner core becomes smallest when the strong eye (IR5) stage is observed.

e. Environmental statistics

Under what environmental conditions do eyes form? From the multitude of SHIPS parameters, we have selected a handful of parameters that characterize the TC environment (see Table 2 for descriptions of these variables and the radii they are averaged over). Bear in mind that many of these parameters are correlated. For instance, regions of high environmental vertical wind shear often occur in the presence of subsidence associated with the shearing upper troughs. It is not our purpose here to conduct a detailed analysis of the changing environment, but rather to provide a basis for understanding the basic environments in which TCs form eyes. Table 7 provides a statistical summary of these parameters at the time that the first aircraft eye was reported (for the values at each individual eye formation event, see Table S6 in the supplement).

1) MAXIMUM POTENTIAL INTENSITY, VMPI

Maximum potential intensity (VMPI) represents the thermodynamic favorableness of the TC environment, with higher potential intensities corresponding to a more favorable thermodynamic environment. For the 70 eye formation cases, VMPI is normally distributed about the median of 133.5 kt (69 m s^{-1}). Half of TCs formed eyes at values between 125 and 145 kt (64 and 74 m s^{-1}). The lowest VMPI at eye formation was 70 kt (36 m s^{-1}), which suggests that eyes do not form in TCs when the thermodynamics cannot support at least a hurricane-strength system.

2) REYNOLDS SEA SURFACE TEMPERATURE, RSST

Eyes tend to form over high SSTs, with a median value of 29.0°C. Only 25% of TCs formed eyes at values lower than 28.5°C. To a large degree, this reflects the fact that many TCs form their eyes at relatively low latitudes in the MDR or in the warm Gulf of Mexico—places where the SST is high. The minimum observed SST of 24°C shows that high SSTs are not essential to eye formation, although low SSTs probably make it less likely.

3) 1000-MB θ_E, E000

The θ_E near the surface (E000) provides an estimate of the energy content of the air that surrounds the TC. Generally, high values of E000 are associated with warm, moisture-rich air—such an environment is conducive to intensification and development of the TC. In contrast, low values of E000 often occur when a deep layer of cool or dry air surrounds the TC. Such an air mass can lead to downdrafts and cold pools that disrupt the convective organization of a TC. A TC may ingest low θ_E air if it entrains warm, dry air off the continent, or if it encounters dry, cool air in association with a cold front. The TCs in the far eastern Atlantic can also ingest low E000 air when they pass near areas of marine stratocumulus clouds.

All eyes formed with a range of E000 values between 321 and 363 K, but the typical range was narrower: 350–356 K. The distribution is skewed toward a small

TABLE 7. Statistical summary of SHIPS environmental parameters at the time of first aircraft eye report (A) for the 70 well observed eye-forming Atlantic TCs (1989–2008). Parameters include maximum potential intensity (VMPI), Reynolds SST (RSST), 1000-mb θ_E (200–800-km average, E000), 200-mb divergence (0–1000-km average, D200), 200-mb temperature (T200), 850–200-mb shear magnitude with vortex removed (0–500-km average, SHDC), and average (0–15 km) vertical velocity of a parcel lifted from the surface (200–800-km average, VVAV).

	Statistics for SHIPS environmental parameters at A						
	VMPI (kt)	RSST (°C)	E000 (K)	D200 (10^{-7} s^{-1})	T200 (°C)	SHDC (kt)	VVAV (m s^{-1})
			Measures of central tendency				
Mean	131.6	28.78	352.4	36.8	−52.76	13.9	12.2
Median	133.5	29.00	353.6	32.1	−52.72	11.7	12.3
			Measures of spread				
Std dev	17.1	1.07	6.5	33.6	0.95	7.4	4.8
IQR	17	0.8	6	43	1.3	10	6
			Measure of symmetry				
Yule–Kendall	0.0	−0.20	−0.2	0.1	−0.06	0.4	−0.1
			Additional measures				
No. of records	70	70	70	70	70	70	70
Max	156	30.6	363	120	−50.9	40	21
75%	142	29.3	356	56	−52.1	19	15
25%	125	28.5	350	13	−53.4	9	9
Min	70	24.0	321	−33	−54.9	4	2

number of considerably lower values. Thus, having energy-rich air in the surrounding environment is not essential to eye formation, but eye formation is less likely when the surrounding air has a low energy content.

4) 200-MB DIVERGENCE, D200

One way to characterize the dynamical forcing in the vicinity of a TC is to consider the large scale 200-mb divergence. Strong divergence at upper levels helps to force broadscale ascent, which supports deep convection. In contrast, weak divergence provides little upward forcing, while convergence leads to downward forcing that tends to inhibit deep convection. The median D200 was 32.1×10^{-7} s^{-1}, with 50% of eyes forming in a range of 13 to 56×10^{-7} s^{-1}. The minimum of -33×10^{-7} s^{-1} shows that an eye can even form when the large-scale environment is convergent at upper levels. Since D200 is averaged over a relatively large area, this large-scale metric may overstate the local convergence over small storms.

5) 200-MB TEMPERATURE, T200

T200 is a near-tropopause reference temperature that impacts a TC's MPI in similar ways as SST, but reversed in sign (for the same SST, a higher 200-mb temperature results in a lower potential intensity). T200 varies with season, latitude, and synoptic regime. T200 temperatures are typically highest over the deep tropics during summer and lowest at high latitudes or in the cores of cold upper lows and upper troughs. The median T200 for our sample is −52.7°C, with a typical range of −53.4° to −52.1°C. While the spread (given by the interquartile range) is just 1.3°C, this is considerably larger than the spread of RSST, which is just 0.6°C. This difference illustrates the greater upper-tropospheric synoptic variability, as compared with the relative homogeneity of the lower tropical troposphere (Malkus 1958).

6) 850–200-MB SHEAR MAGNITUDE, SHDC

Environmental vertical wind shear can be difficult to quantify over the TC, and the SHIPS dataset includes several different measures. We chose SHDC, which is a standard measure of the deep shear. In our sample, the median vertical shear at the time of eye formation is 11.7 kt (6.0 m s^{-1}). The Yule–Kendall index, a robust measure of the symmetry of the distribution, shows that the distribution is skewed considerably toward high shear values. Indeed, the mean of the distribution [13.9 kt (7.2 m s^{-1})] is substantially above the median. The middle 50% of TCs form eyes under vertical shears ranging from 9 to 19 kt (4.6 to 9.8 m s^{-1}).

A bit of caution should be taken in interpreting the extrema of the SHDC distribution. The minimum of 4 kt (2 m s^{-1}) should not be taken to mean that eyes cannot form in a zero-shear environment. Rather, this likely reflects the impact of the large averaging radius. Area-mean shear values lower than this value rarely exist in the presence of a TC over a radius of this size. Likewise, the maximum value should not be taken to mean that eyes can generally form at vertical shears up to 40 kt (21 m s^{-1})—in such cases, areas of high shear were

undoubtedly occurring within 500 km of the TC center, but it is possible that the high shear did not directly impinge on the TC's inner core. This latter situation can occur when the TC is smaller than the averaging radius.

7) VERTICAL VELOCITY OF A PARCEL LIFTED FROM THE SURFACE, VVAV

The last environmental parameter measures the convective instability of a parcel lifted from the surface. High VVAV values indicate that a lifted parcel is conditionally unstable and could lead to vigorous convective updrafts. Low VVAV values indicate low instability and the potential for just weak updrafts. The eyes in this sample form at a median VVAV of 12.3 m s^{-1}, with a typical range of 9–15 m s^{-1}. While even the maximum value of 21 m s^{-1} may seem low compared with midlatitude convection (which can have calculated updrafts exceeding 80 m s^{-1}), these values suggest that eyes form when the environment contains air parcels that have a moderate degree of convective instability. The minimum value of 2 m s^{-1} shows that instability is not essential, however.

To sum up, Atlantic TCs form eyes in environments that are thermodynamically supportive of moderate-to-high potential intensity [VMPI $\geq$ 125 kt (64.3 m s^{-1})]. Such environments typically include high SSTs (RSST $\geq$ 28.5°C), energy-rich air in the surroundings that is not too dry or cool (E000 $\geq$ 350 K), and relatively colder temperatures at 200 mb (T200 ≤ -52.1°C). Eye formation is also favored in environments that are divergent in the upper levels (D200 $\geq 13 \times 10^{-7}$ s^{-1}), environments that are convectively unstable (VVAV $\geq$ 9 m s^{-1}), and environments that are not strongly sheared [SHDC $\leq$ 19 kt (9.8 m s^{-1})].

f. Spatial distribution

Figure 4 presents the spatial distribution of eye formations stratified by the case types: rapid dissipation, intermittent formation, delayed formation, and sustained formation. Each panel displays the best tracks corresponding to TCs of a particular case type. For reference, Fig. 5 provides the storm names for the TCs in each case type.

Figure 4a shows the tracks of the 17 rapid dissipation cases. Rapid eye dissipation occurs more frequently in early and late season TCs. One cluster of irregular, meandering tracks off the U.S. East Coast suggests TCs of subtropical origin. From a review of the satellite imagery, these TCs often have well-defined surface circulations, but struggle to close off enough deep convection to meet the definition for an eyewall. Six of the other rapid dissipation cases formed eyes in the Gulf of Mexico, but at least three of these TCs had their eye developments arrested by landfall.

Figure 4b displays the 24 intermittent formation cases. Four of these TCs formed eyes and were likely developing but then hit the Gulf Coast. Another subset of TCs formed short-lived eyes near the Leeward Islands. The midoceanic tropical tropospheric upper trough (TUTT) has a mean summer position in this area (Sadler 1976; Fitzpatrick et al. 1995), so the eye formations of these TCs may have been disrupted by adverse environmental vertical wind shear, subsidence, and higher sea level pressures (Knaff 1997).

Figure 4c shows the 12 delayed formation cases. The broad, sweeping tracks of these TCs suggest a favorable upper-level environment (an absence of shearing troughs or cold lows) and/or the presence of a midtropospheric ridge. When such a ridge lies to the north of the TC, it provides a consistent steering environment. Nevertheless, temporarily hostile conditions or disruptive internal dynamics can still lead to setbacks.

Figure 4d shows the tracks of the 17 TCs with sustained formation. As in the delayed formation cases, many of these TCs have straight-running or broadly curving tracks, which suggests favorable environments. A significant cluster of TCs originate in the western Caribbean, however, and have low-latitude recurving tracks. These tracks are from late-season TCs (e.g., Mitch 1998, Michelle 2001, and Paloma 2008) that rapidly developed and then recurved into the westerlies.

Interestingly, both the delayed formation and sustained formation cases have a distinct absence of the irregular tracks typical of TCs forming in the subtropics. During the subjective analysis of the IR archive, we noticed that several subtropical systems did form eyes in the eastern Atlantic, but since these TCs were not reconnoitered by aircraft they do not appear in the present climatology.

Landfall does not always prevent eye formation. Figure 4b shows the track of Fay (2008), which hit southwest Florida just after forming an open aircraft eye. While over south Florida, a distinct satellite eye appeared and persisted until after the TC moved back over water. Several other systems also seem to have formed their first satellite eyes (IR3) while over land (see filled squares over the Yucatan Peninsula, Nicaragua, and the Mississippi River delta).

g. Temporal distribution

We now turn our attention to the temporal distribution of eye development during the TC life cycle. To compare the eye formations of this diverse set of TCs, it helps to choose a common reference time point. Taking this point to be the time when each TC first reaches tropical storm intensity [BT $v_{max} > 34$ kt (17.5 m s^{-1})], this reference time has been subtracted from the time of

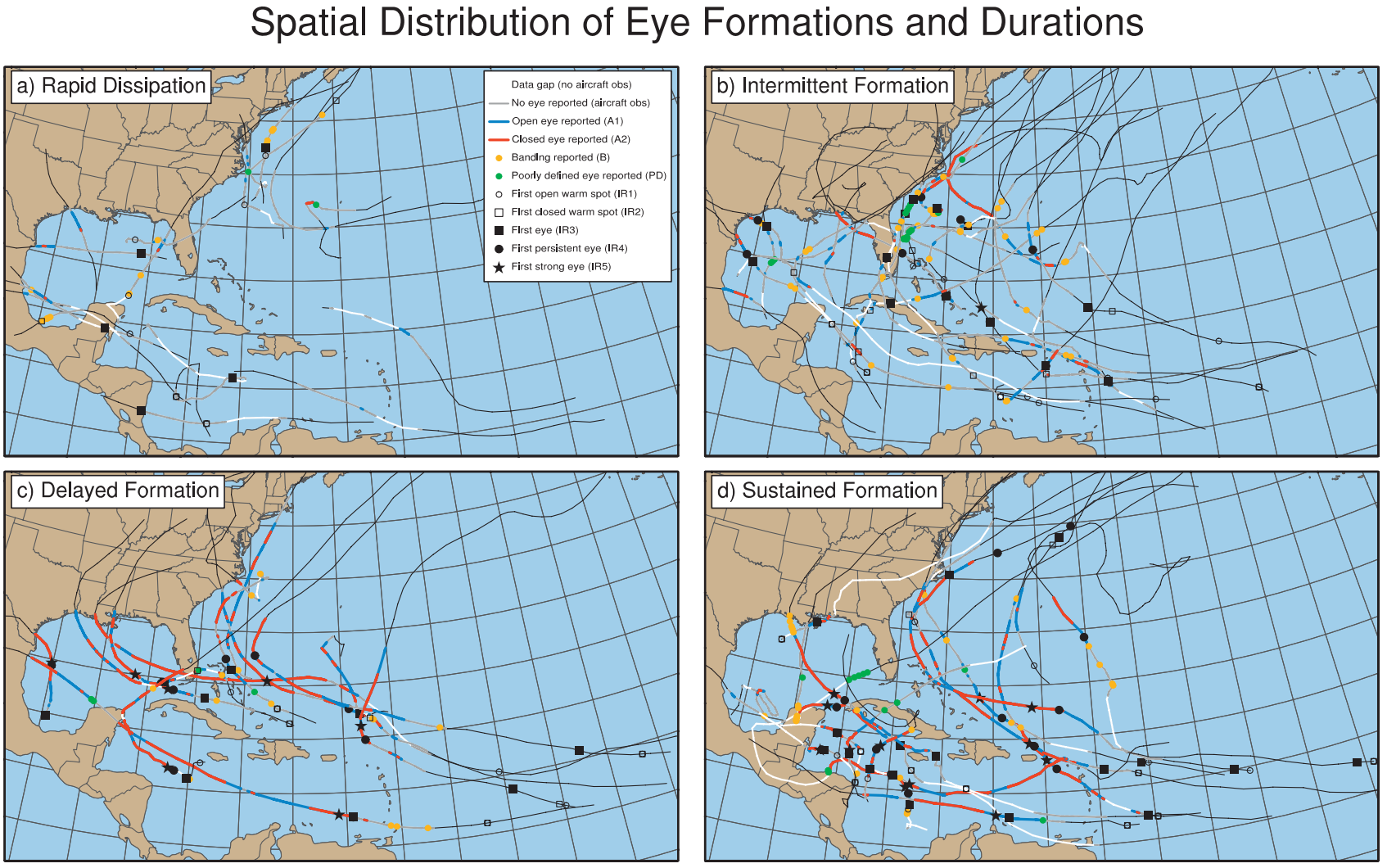

FIG. 4. Spatial distribution of all Atlantic TCs that formed eyes during the period of aircraft reconnaissance. Best tracks correspond to TCs from the following case types: (a) "rapid dissipation," (b) "intermittent formation," (c) "delayed formation," and (d) "sustained formation." Line colors for each track segment indicate the following: periods before and after the period of aircraft reconnaissance (black), data gaps of 12 h or greater that occurred *within* the reconnaissance period (white), periods when the TC was regularly reconnoitered, but an eye was not reported (gray), periods of active reconnaissance when an open eye was reported (blue), and likewise, periods when aircraft reported a closed eye (red). Orange dots indicate specific fixes in which aircraft reported banding (but not an eye), while green dots indicate fixes in which a poorly defined eye was reported. Additionally, polymarkers indicate the locations when a TC first attained the following stages of IR eye development: open warm spot (IR1, hollow circle), closed warm spot (IR2, hollow square), first eye (IR3, filled square), first persistent eye (IR4, filled circle), and the first strong eye (IR5, filled star).

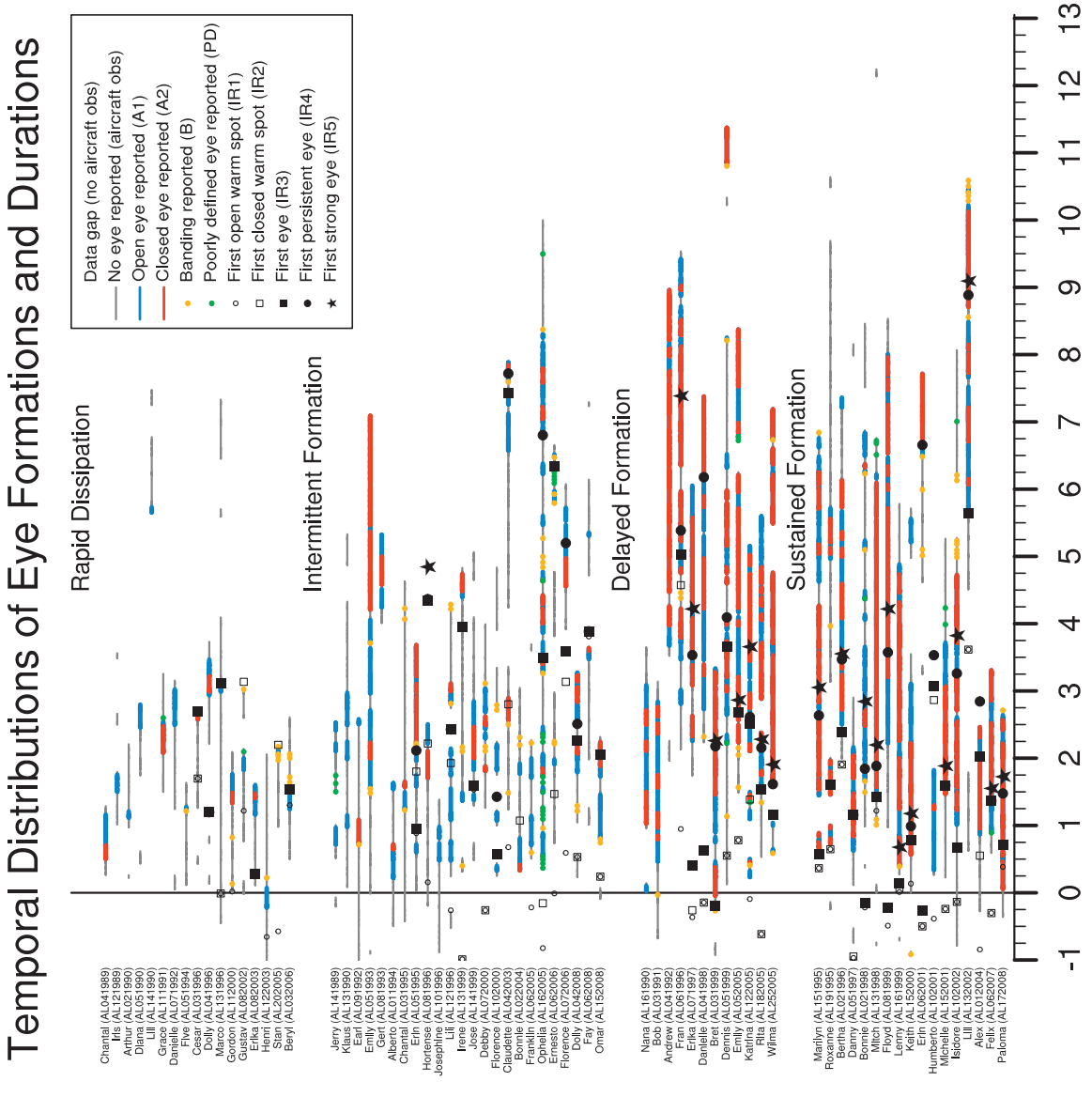

FIG. 5. Temporal distribution of all Atlantic TCs that formed eyes during the period of aircraft reconnaissance. Conventions are the same as in Fig. 4.

each eye development baseline for each of the 70 eye-forming storms. This allows a timeline to be constructed for each TC, showing the relative timing of the eye development stages in days since the TC reached tropical storm status. The resulting montage of timelines is shown in Fig. 5, grouped by case type.

Starting with the 17 rapid dissipation cases, it is immediately evident that many of these TCs were only observed by aircraft for a few days and that all of their eye formations were brief (this must be the case, by the definition of this case type). While many of these TCs did form satellite eyes (IR3), none of them reached the persistent eye (IR4) or strong eye (IR5) stages. While this case type does not include reformation cases, the scattered presence of banding (orange dots) indicates that some TCs possessed incomplete eye structure for longer periods of time.

The 24 TCs that experienced intermittent eye formation generally lasted longer than those in which the eye rapidly dissipated, but the vast majority of these TCs did not become intense. Some intermittent formation TCs eventually did form eyes that lasted longer than the 24-h criterion, albeit outside of the 3-day time window from the initial aircraft eye report. In most of the intermittent formation TCs, aircraft first reported an open eye (A1)—this suggests that the initial eyes of these TCs were marginally defined. Even though the initial eye formations were intermittent in these cases, persistent satellite eyes (IR4) were eventually noted in 7 of the 17 TCs (41.2%) that had satellite coverage, while 1 TC even developed a strong eye (IR5, 5.9%). Taken together, these timelines suggest slowly developing systems that had difficulty forming an eye. Some TCs eventually formed sustained eyes long after the 3-day window. As an example, Ophelia (2005) took nearly eight days from the first hint of an eye (open warm spot, IR1) to IR4. However, few TCs with intermittent eye formation ever become major hurricanes.

The 12 delayed formation cases were longer lived, became more intense, and in some cases, showed signs of eye development a day or two before aircraft observations began. Nevertheless, all of these TCs had their eye developments interrupted by some inhibiting factor. Once this inhibition was removed, the TCs developed consistently and in some cases rapidly. Indeed, some of these TCs took longer to form eyes after reaching tropical storm intensity (even 3 or 4 days in some cases). This bolsters the view that the environment or some other factor was initially unfavorable for development. Of the nine delayed formation cases with sufficient satellite coverage, all formed IR4 eyes and seven (77.8%) formed IR5 eyes. Nine of the 12 (75%) delayed formation cases became major hurricanes.

In contrast to the delayed formation cases, the 17 sustained formation cases often formed eyes within a day of attaining tropical storm strength and 15 of them (88%) became major hurricanes. In many of these cases, the first reported aircraft eye was closed (A2), so not only did these TCs form eyes quickly, but their eyes were better defined when they appeared. Some of these TCs rapidly intensified, progressing all the way to an IR5 eye within a day of first forming an eye. Of these cases, 14 (82.3%) reached the IR4 stage, and 12 (70.6%) continued to the IR5 stage. All of this suggests that these TCs developed in a very favorable environment. All sustained formation cases also formed from 1995 onward, an era of more frequent and intense hurricanes (Goldenberg et al. 2001).

Surprisingly, more than half the sustained formation cases displayed open or closed warm spots (IR1 and IR2) and even actual eyes (IR3) *before* the TCs reached tropical-storm intensity. In our view, these ''extra-early formers'' may represent a special class of eye formation distinct from normal development. Perhaps the best example of an extra-early former is Erin (2001), which formed an IR3 eye in the far eastern Atlantic just as it was designated as a tropical depression. A distinct warm spot surrounded by a ring of curved deep convection appeared and persisted for several hours before being obscured by deep convection. Erin continued to display some signs of eye structure for several more hours, but then came under hostile vertical wind shear. Almost a week later, the TC reached the IR4 stage and developed into a major hurricane.

h. Timing between aircraft and satellite eye detection

Which comes first—the aircraft eye or the satellite eye? A careful inspection of Fig. 5 reveals information about the relative timing of the first aircraft eye (A) versus the first satellite eye (IR3). Since eye structure often forms beneath an obscuring central dense overcast, we might generally expect that aircraft would detect the eye *before* it appears in the upper cloud field. To show whether the data support this expectation, it is necessary to remove from consideration any cases for which satellite data were unavailable, as well as cases that were not yet under aircraft surveillance by the time a satellite eye was noted. Of the 43 remaining cases, the aircraft eye was observed first in 36 TCs (83%), while the satellite eye was observed first in just 7 TCs (17%). Hence, in an overwhelming majority of cases, the eye was observed first by aircraft.

i. Time needed to achieve each stage of eye development

By using the time when a TC first reaches tropical storm status as a reference point, the length of time

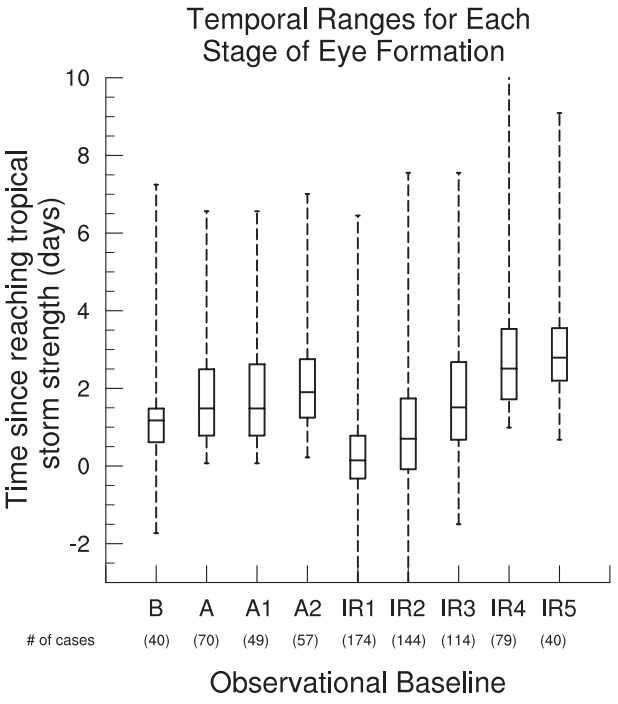

FIG. 6. Box-and-whisker plot showing the temporal ranges of time needed for TCs to achieve each eye development baseline. Times are given in days since the TC first reached tropical storm intensity [BT $v_{max} > 34$ kt (17.5 m s^{-1})]. The center line of each box gives the median value, while the top and bottom box edges correspond to the top and bottom hinges of the distribution (hinges are nearly the same as the quartiles of the distribution). The endpoints of the whiskers correspond to the extreme values of the distribution. Plot range is truncated to focus on the most common values, but extrema range between −5.8 and 18.3 days.

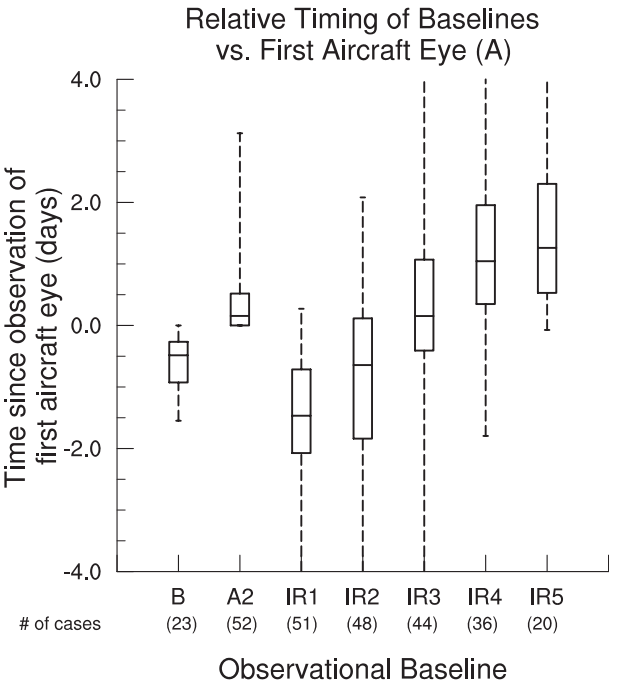

FIG. 7. As in Fig. 6, but for the relative timing differences between each of the eye development baselines and the first aircraft eye (A). Plot range has been truncated.

needed to achieve each eye development baseline is computed. Figure 6 displays a histogram summarizing the statistics of these relative timings. Using the median value to represent the center of the distribution, the following median timings are obtained (each number in parentheses indicates the median time, in hours, that the TC took to reach the designated eye development baseline since becoming a tropical storm): A1 (35.6 h), IR3 (36.7 h), A2 (45.6 h), IR4 (61.2 h), and IR5 (68.3 h). Fifty percent of TCs formed their first aircraft eye within 18.8–60.0 h of becoming a tropical storm. In fact, 34% of the 70 TCs in this climatology formed an eye within the first 24 h of reaching tropical storm status, 67% formed eyes by 48 h, and 89% formed eyes by 72 h. Taken together, these data suggest that there is an opportune time window of approximately a day or two during which a young tropical storm can readily form an eye. Very few TCs were observed to form eyes more than 5 days after becoming a tropical storm. Apparently, after three or more days of eyeless-ness a TC is much less likely to form an eye.

j. Characteristic time scale for eye development

What is the characteristic time scale for eye development? To answer this, it is instructive to compare the relative timing between the first aircraft eye observation and the appearance of the other eye development baselines. We obtain this by subtracting the time when the aircraft eye was first observed (A) from the time of the other eye development baselines. The distributions of these relative timing data are presented as a histogram in Fig. 7. If these median timings can be taken to represent a ''median TC,'' the IR3 eye appears 3.6 h after A, while IR4 and IR5 are reached 25.1 and 30.3 h after A. Banding (B) is typically reported 11.6 h *before* A. Accounting for the latency difference between aircraft fixes (approximately 4 h) and satellite images (30 min), the 3.6-h difference between A and IR3 suggests a 7-h lag between the observation of an aircraft eye and the appearance of eyelike structure (IR3) in the upper cloud field. Taken together, if the full development of the eye is considered to include the stages from banding through IR4, then the characteristic time scale for eye development is about 36 h.

Further information can be obtained by computing the empirical cumulative frequency distribution of the elapsed time to eye formation (Fig. 8). Only 12% of TCs formed eyes 18 h after becoming a tropical storm, but by

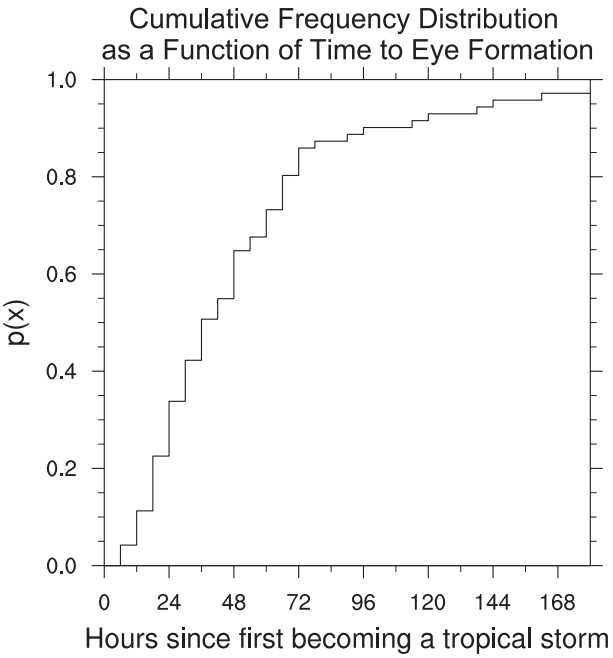

FIG. 8. Cumulative frequency distribution of the probability of forming an eye. Time is measured relative to the first point that a system becomes a tropical storm according to the best track. The time of eye formation is taken to be the first report of an aircraft eye (A).

48 h, fully 65% of TCs have formed eyes. Thus, more than 50% of TCs form eyes between 18 and 48 h of becoming a tropical storm. The cumulative frequencies continue to rise steadily until about 72 h when the rate of increase slows markedly. This steep initial rise, coupled with the slow tail-off, give the distribution a distinct concave-downward shape. This indicates that the data are skewed toward long elapsed times. That is, a small number of TCs take considerably longer to form eyes than the vast majority of cases.

We interpret these data to suggest that the initial eye formation depends largely on the TC being in a favorable environment mostly devoid of negative influences. Since many TCs undergo genesis in a favorable environment, they form eyes as soon as they can so long as conditions remain favorable. A few TCs take much longer to form their eyes, presumably because these TCs encounter hostile environments before their eyes are able to form. So long as the environment remains unfavorable, eye formation may be delayed (or precluded).

7. Summary and conclusions

The purpose of this study has been to provide a comprehensive climatology of hurricane eye formation. To accomplish this, we synthesized a new structure and intensity dataset from over 4600 VDMs, the BT and EBT datasets, and the SHIPS development dataset. Together with the IR archive, we analyzed these data to determine the times at which each eye development baseline was observed. Of the 183 TCs that were reconnoitered in the North Atlantic basin between 1989 and 2008, 70 TCs formed eyes and possessed sufficient data to be included as cases. The major findings of the climatology are now summarized.

1) **Banding is a precursor to eye formation.** Aircraft reports of banding are fairly common, occurring in 43% of all Atlantic TCs. Of the 62 TCs that displayed banding prior to the formation of any eye, 51% later developed an aircraft eye.
2) **About 60% of TCs develop an eye during their lifetime.** An aircraft eye was reported in 59% of reconnoitered TCs, while 61% of satellite-observed TCs displayed a satellite eye (IR3). As one might expect, closed aircraft eyes (47%) were less frequently observed than open aircraft eyes (58%). Only 43% of TCs developed a persistent eye (IR4), and just 21% achieved a strong eye (IR5). Of the TCs that were observed by both aircraft and satellite, eye structure was observed more frequently by satellite (IR3, 67%) than by aircraft (A, 58%). Taking countervailing sampling and detection factors into account, we estimate the true frequency of eye formation to be about 60% for all TCs across the basin. This is somewhat higher than the total proportion of TCs that become hurricanes (52%).
3) **Eyes are more likely to be seen first by aircraft than satellite.** It has been generally thought that the convective ring of the developing eyewall should be apparent to aircraft before the eye is observed by satellite. This was indeed the case: for the TCs observed by both aircraft and satellite, the aircraft eye was reported before the satellite eye (IR3) in most cases (83%). This suggests that eye structure may develop first at lower levels (where it is more likely to be reported as an aircraft eye). Only later does the eye structure usually become observable in the cloud field (as seen from above). A few TCs (17%) develop eye structure in the cloud field before it is observed by aircraft. In such cases, it seems that the eye structure developed concurrently through the depth of the TC.
4) **Aircraft eyes form at intensities that are considerably lower than hurricane intensity.** Aircraft reported the first eyes at a wide range of intensities, but the median BT v_{max} is 58 kt (30 m s^{-1}). This key finding may seem to contravene the conventional wisdom that the appearance of an eye marks the cyclone's crossing of the hurricane intensity threshold;

however, this result is still broadly consistent with the Dvorak technique under the interpretation that the formation of a lower-tropospheric convective ring likely occurs well before the upper-tropospheric subsidence is strong enough to clear out the eye. We will give a more detailed discussion of this issue in a follow-up study on the intensity ranges and changes that occur during the eye formation process.

5) **Eyes tend to form in environments that are conducive to further intensification of the TC.** Eye formation is favored when potential intensities are large, a situation that occurs with high SSTs and correspondingly low upper-level temperatures. Eye formation is also favored when the environmental vertical wind shear is low to moderate, when the surrounding surface air is not too cool or dry, when the large-scale environment favors moderate to strong divergence aloft, and when air parcels are convectively unstable.
6) **TCs that form aircraft eyes tend to do so quickly after reaching tropical storm threshold.** The temporal distribution of observed eye development baselines shows that most (67%) TCs that form eyes tend to do so within 48 h of reaching tropical storm strength. This is consistent with the Dvorak model of development, in which the typical TC strengthens from a T number of 2.5 to 4.5 over 2 days [with a corresponding intensity increase from 35 to 77 kt (18 to 40 m s^{-1})]. Our results suggest that there is about a 1- or 2-day time window during which a TC that has undergone genesis can quickly form an eye. If environmental conditions are unfavorable so that the initial eye dissipates, the TC may take several more days to reform an eye. However, rapid dissipation of the initial eye is not necessarily detrimental—while a sizable subset of TCs form eyes that do not persist initially, if the eye reforms within a day or so, many of these TCs begin to develop rapidly. This behavior suggests that environmental conditions play a key role in the longevity and persistence of the eye/eyewall structure. If and when adverse conditions improve, development can be rapid.

In closing, we suggest other possible uses of the VDM dataset. Besides eye formation, these data could be used to study structural changes at other stages of the TC life cycle, such as eyewall replacement cycles or peak intensity. These data could even be used to delve into the somewhat rare occurrence in which the TC takes on a *warm ring* structure, as opposed to the more typical *warm core* structure (Schubert et al. 2007). For such a problem, the VDM data can serve as a road map by identifying warm ring cases; this would facilitate a more detailed investigation of the full flight level data.

Many real-time applications can be envisaged if the aircraft-based structure and intensity parameters are made available in real time. Such data could support the development of statistical-dynamical forecast aids for structure and size. Kossin and Sitkowski (2009) developed an empirical method to predict secondary eyewall formation using environmental and satellite parameters. While they noted that their prediction method could be refined using high temporal frequency aircraft reconnaissance observations, they did not attempt to do so because these data were not available in a convenient format. To fill this gap, we are working to release a development version of the VDM-based structure and intensity dataset as well as an updating real-time component. We believe that the incorporation of these structure data will yield more accurate predictions of both intensity and structure.

Acknowledgments. We owe an enormous debt to the brave flight crews of the 53rd Weather Reconnaissance Squadron and NOAA's Aircraft Operation Center who put themselves at risk each time they collect these vital data. Without their dedication and diligence, this study would not have been possible. We thank Steve Feuer, A. Barry Damiano, John Pavone, Chris Sisko, Christopher Juckins, Mark Zimmer, Christopher Landsea, and Neal Dorst for their assistance in obtaining the many VDM messages. They, along with Eric Blake, Jonathan Talbot, Jack Parrish, and Nicholas Carrasco, graciously answered our many questions about the VDM contents, history, and usage. Buck Sampson and James Franklin provided information about the ATCF b-decks. We thank Ray Zehr and Mark DeMaria for their insightful suggestions, and Mary Haley and David Brown for their programming advice. Chris Davis, George Bryan, Chris Rozoff, and an anonymous reviewer provided helpful comments that led to improvements in the manuscript. The first author gratefully acknowledges the support of the Advanced Study Program and the NCAR Earth System Laboratory. This research was supported by NASA/TCSP Grant NNG06GA54G and by NSF Grants ATM-0332197 and ATM-0837932.

REFERENCES

Anthes, R. A., 1982: *Tropical Cyclones: Their Evolution, Structure, and Effects. Meteor. Monogr.,* No. 41, Amer. Meteor. Soc., 208 pp.

Ballou, S. M., 1892: The eye of the storm. *Amer. Meteor. J.,* **9** (2), 67–84, 121–127.

Bister, M., and K. A. Emanuel, 1998: Dissipative heating and hurricane intensity. *Meteor. Atmos. Phys.,* **65,** 233–240.

DeMaria, M., and J. Kaplan, 1994: A Statistical Hurricane Intensity Prediction Scheme (SHIPS) for the Atlantic basin. *Wea. Forecasting,* **9,** 209–220.

——, and ——, 1999: An updated Statistical Hurricane Intensity Prediction Scheme (SHIPS) for the Atlantic and eastern North Pacific basins. *Wea. Forecasting,* **14,** 326–337.

——, M. Mainelli, L. K. Shay, J. A. Knaff, and J. Kaplan, 2005: Further improvements to the Statistical Hurricane Intensity Prediction Scheme (SHIPS). *Wea. Forecasting,* **20,** 531–543.

Demuth, J. L., M. DeMaria, and J. A. Knaff, 2006: Improvement of Advanced Microwave Sounding Unit tropical cyclone intensity and size estimation algorithms. *J. Appl. Meteor. Climatol.,* **45,** 1573–1581.

Dvorak, V. F., 1984: Tropical cyclone intensity analysis using satellite data. NOAA Tech. Rep. NESDIS 11, Washington, DC, 47 pp.

Fitzpatrick, P. J., 1996: Understanding and forecasting tropical cyclone intensity change. Dept. of Atmospheric Science Paper 598, Colorado State University, 346 pp. [Available from Dept. of Atmospheric Science, Colorado State University, Fort Collins, CO 80523.]

——, J. A. Knaff, C. W. Landsea, and S. V. Finley, 1995: Documentation of a systematic bias in the Aviation Model's forecast of the Atlantic Tropical Upper Tropospheric Trough: Implications for tropical cyclone forecasting. *Wea. Forecasting,* **10,** 433–446.

Franklin, J. L., M. L. Black, and K. Valde, 2003: GPS dropwindsone wind profiles in hurricanes and their operational implications. *Wea. Forecasting,* **18,** 32–44.

Goldenberg, S. B., C. W. Landsea, A. M. Mestas-Nuñez, and W. M. Gray, 2001: The recent increase in Atlantic hurricane activity: Causes and implications. *Science,* **293,** 474–479.

Gray, W. M., and D. J. Shea, 1973: The hurricane's inner core region. II. Thermal stability and dynamic constraints. *J. Atmos. Sci.,* **30,** 1565–1576.

Jorgensen, D. P., 1984a: Mesoscale and convective-scale characteristics of mature hurricanes. Part I: General observations by research aircraft. *J. Atmos. Sci.,* **41,** 1268–1285.

——, 1984b: Mesoscale and convective-scale characteristics of mature hurricanes. Part II: Inner core structure of Hurricane Allen (1980). *J. Atmos. Sci.,* **41,** 1287–1311.

Kimball, S. K., and M. S. Mulekar, 2004: A 15-year climatology of North Atlantic tropical cyclones. Part I: Size parameters. *J. Climate,* **17,** 3555–3575.

Knaff, J. A., 1997: Implications of summertime sea level pressure anomalies in the tropical Atlantic region. *J. Climate,* **10,** 789–804.

——, D. P. Brown, J. Courtney, G. M. Gallina, and J. L. Beven II, 2010: An evaluation of Dvorak technique-based tropical cyclone intensity estimates. *Wea. Forecasting,* **25,** 1362–1379.

Kossin, J. P., and M. Sitkowski, 2009: An objective model for identifying secondary eyewall formation in hurricanes. *Mon. Wea. Rev.,* **137,** 876–892.

Malkus, J. S., 1958: Tropical weather disturbances—Why do so few become hurricanes. *Weather,* **13,** 75–89.

McAdie, C. J., C. W. Landsea, C. J. Neumann, J. E. David, E. S. Blake, and G. R. Hammer, 2009: *Tropical Cyclones of the North Atlantic, 1851–2006.* 6th ed. Historical Climatology Series 6-2, NCDC, 238 pp. [Available from the National Climatic Data Center, 151 Patton Ave., Room 120, Asheville, NC 28801-5001. Also available online at http://www.nhc.noaa.gov/abouttrackbooks.shtml.]

Mundell, D. B., 1990: Prediction of tropical cyclone rapid intensification. M.S. thesis, Dept. of Atmospheric Science, Colorado State University, 186 pp.

Olander, T. L., and C. S. Velden, 2007: The Advanced Dvorak Technique: Continued development of an objective scheme to estimate tropical cyclone intensity using geostationary infrared satellite imagery. *Wea. Forecasting,* **22,** 287–298.

Palmén, E., 1956: Formation and development of tropical cyclones. *Proc. Tropical Cyclone Symp.,* Brisbane, Australia, Australian Bureau of Meteorology, Paper 13, 213–231.

Powell, M. D., E. W. Uhlhorn, and J. D. Kepert, 2009: Estimating maximum surface winds from hurricane reconnaissance measurements. *Wea. Forecasting,* **24,** 868–883.

Sadler, J. C., 1976: A role of the tropical upper tropospheric trough in early season typhoon development. *Mon. Wea. Rev.,* **104,** 1266–1278.

Sampson, C. R., and A. J. Schrader, 2000: The automated tropical cyclone forecasting system (version 3.2). *Bull. Amer. Meteor. Soc.,* **81,** 1231–1240.

Schubert, W. H., and J. J. Hack, 1982: Inertial stability and tropical cyclone development. *J. Atmos. Sci.,* **39,** 1687–1697.

——, C. M. Rozoff, J. L. Vigh, B. D. McNoldy, and J. P. Kossin, 2007: On the distribution of subsidence in the hurricane eye. *Quart. J. Roy. Meteor. Soc.,* **133,** 595–605, doi:10.1002/qj.49.

Shapiro, L. J., 1983: The asynmmetric boundary layer flow under a translating hurricane. *J. Atmos. Sci.,* **40,** 1984–1998.

——, and H. E. Willoughby, 1982: The response of balanced hurricanes to local sources of heat and momentum. *J. Atmos. Sci.,* **39,** 378–394.

Shea, D. J., and W. M. Gray, 1973: The hurricane's inner core region. I. Symmetric and asymmetric structure. *J. Atmos. Sci.,* **30,** 1544–1564.

Smith, R. K., 1981: The cyclostrophic adjustment of vortices with applications to tropical cyclone modification. *J. Atmos. Sci.,* **38,** 2021–2030.

Stern, D. P., and D. S. Nolan, 2011: On the vertical decay of the maximum tangential winds in tropical cyclones. *J. Atmos. Sci.,* **68,** 2073–2094.

Vigh, J. L., 2010: Formation of the hurricane eye. Ph.D. dissertation, Colorado State University, 538 pp. [Available online at http://hdl.handle.net/10217/39054.]

Weatherford, C. L., and W. M. Gray, 1988a: Typhoon structure as revealed by aircraft reconnaissance. Part I: Data analysis and climatology. *Mon. Wea. Rev.,* **116,** 1032–1043.

——, and ——, 1988b: Typhoon structure as revealed by aircraft reconnaissance. Part II: Structural variability. *Mon. Wea. Rev.,* **116,** 1044–1056.

Willoughby, H. E., 1990: Temporal changes of the primary circulation in tropical cyclones. *J. Atmos. Sci.,* **47,** 242–264.

Yanai, M., 1961: A detailed analysis of typhoon formation. *J. Meteor. Soc. Japan,* **39,** 187–214.

Zehr, R. M., and J. A. Knaff, 2007: Atlantic major hurricanes, 1995–2005—Characteristics based on best-track, aircraft, and IR images. *J. Climate,* **20,** 5865–5888.